Electronic Supplementary Information

Influence of Ruthenium Substitution in $LaCoO_3$ towards Bi-functional Electrocatalytic activity for Rechargeable Zn-Air Battery

Shivaraju Guddehalli Chandrappa,[a,b,c] Prabu Moni,[a,b] Dehong Chen,[c] Guruprakash Karkera,[a,b] Kunkanadu R Prakasha,[a,b] Rachel A. Caruso,[c] and Annigere S. Prakash*[a,b]

Table S1. Crystallographic parameters for $LaCo_{1-x}Ru_xO_3$ (x = 0.0, 0.2, 0.3 and 0.5) determined from Rietveld refinement of powder x-ray diffraction patterns.

x	Space group	a Å	b Å	c Å	V Å^3	La (x y z)	Co, Ru (x y z)	O1 (x y z)	O2 (x y z)	R_{wp} %	χ^2
0	$R\bar{3}c$	5.442(4)	5.442(4)	13.099(1)	336.01	0.0000 0.0000 0.2500	0.0000 0.0000 0.0000	0.45133 0.0000 0.25000		9.66	3.46
0.2	$R\bar{3}c$	5.521(4)	5.521(4)	13.335(2)	352.06	0.0000 0.0000 0.2500	0.0000 0.0000 0.0000	0.45141 0.0000 0.25000		15.0	4.63
0.3	$R\bar{3}c$	5.528(9)	5.528(9)	13.474(6)	356.71	0.0000 0.0000 0.2500	0.0000 0.0000 0.0000	0.45756 0.0000 0.25000		12.5	4.70
	Pbnm	5.565(6)	5.553(2)	7.858(8)	242.89	0.52372 0.46324 0.25000	0.50000 0.0000 0.00000	0.53815 0.06166 0.25000	0.85319 0.18651 0.01711		
0.5	*Pbnm*	5.573(5)	5.638(0)	7.886(8)	247.83	0.51818 0.45521 0.25000	0.50000 0.00000 0.0000	0.45180 0.01574 0.25000	0.77348 0.21758 0.05963	11.7	4.14

i) Electrochemical Measurements

The electron transfer number per oxygen molecule (*n*) calculated from Koutecky-Levich (K-L) plots were determined by follow equation:

$$\frac{1}{J} = \frac{1}{J_k} + \frac{1}{B\omega^{1/2}}$$

Where j is the measured current density, jk is the kinetic current density and ω is the angular velocity of the disk (ω=2πN, N is the linear rotation speed).

$$B = 0.62nFC_{O2}(D_{O2})^{2/3}\gamma^{-1/6}$$

Where, n represents the overall number of electrons gained per oxygen, F is the Faraday constant (F= 96485 C mol^{-1}), C_{O2} is the bulk concentration of O_2 (1.21×10^{-3} mol L^{-1}), D_{O2} is the diffusion coefficient of O_2 in 0.1 M KOH electrolyte (1.86×10^{-5} cm^2 s^{-1}), *γ* is the kinetic viscosity of the electrolyte (1.009×10^{-2} cm^2 s^{-1}.

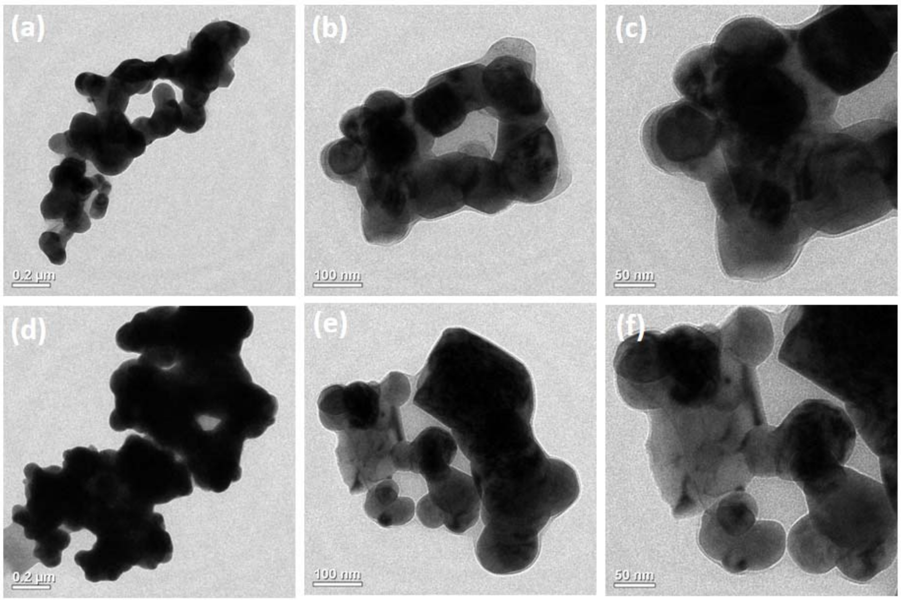

Fig. S1 TEM images of **(a-c)** LCO and **(d-f)** LCRO82.

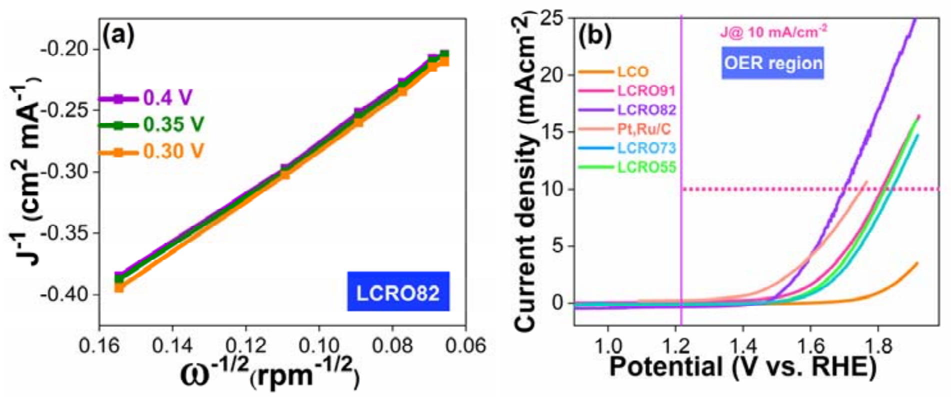

Fig. S2 (a) *K–L plots of the LCRO82 catalyst,* ***(b)*** *OER activity of* $LaCo_{1-x}Ru_xO_{3-\delta}$ *(x=0, 0.2, 0.3 and 0.5) and Pt, Ru/C catalysts. (IR corrected).*

ii) Determination of Oxygen vacancy:

The oxygen non-stoichiometry ($\boldsymbol{\delta}$) of prepared LCO and LCRO82 catalysts were measured using iodometric titration method (the detailed titration procedures are in the below cited reference) and the amount of oxygen non-stoichiometry ($\boldsymbol{\delta}$) was calculated using the below-mentioned formula.[1]

$$\boldsymbol{\delta} = \frac{(4 - Y)m - M}{2m - 16n}$$

where n = C × ΔV

M = Molar mass of the sample

C = Concentration of $Na_2S_2O_3$

Y = Average valence state of B site

ΔV = Total consumption Volume of $Na_2S_2O_3$ solution

m = Sample mass

Table S2. Calculated $\boldsymbol{\delta}$ value of LCO and LCRO82.

Sample	**ΔV in mL**	$\boldsymbol{\delta}$
LCRO82	3.6	0.31
LCO	4.3	0.23

iii) XPS data

Table S3. XPS binding energy data for LCO and LCRO82 catalysts.

Sample	**La 3d**	**Co 2p**	**O 1s**	**Ru 3p**	**Ru 3d**
LCO	3d $_{5/2}$: 833.57 eV 3d $_{3/2}$: 849.86 eV	**2 P$_{3/2}$:** 780.91 eV (Co^{2+}) 779.56 eV (Co^{3+}) **2 P$_{1/2}$:** 796.12 eV (Co^{2+}) 794.71 eV (Co^{3+})	528.74 eV	-	-
LCRO82	3d $_{5/2}$: 833.82 eV 3d $_{3/2}$: 850.07 eV	**2 P$_{3/2}$:** 780.49 eV (Co^{2+}) 779.22 eV (Co^{3+}) **2 P$_{1/2}$:** 795.99 eV (Co^{2+}) 794.72 eV (Co^{3+})	528.78 eV	2 P$_{3/2}$: 464.27 eV and 2 P$_{1/2}$:486.55 eV	3d $_{5/2}$:282.48 eV and 3d $_{3/2}$:286.58 eV

Table S4. The relative amounts of different Co species in the LCO and LCRO82 samples (obtained from area under fitted XPS peaks).

Sample	**Co^{2+} 2 P$_{1/2}$**			**Co^{3+} 2 P$_{1/2}$**			**Co^{2+} 2 P$_{3/2}$**			**Co^{3+} 2 P$_{3/2}$**			**Co^{2+}/Co^{3+} ratio**
	Peak position	**FWHM**	**Area**	**Peak position**	**FWHM**	**Area**	**Peak position**	**FWHM**	**Area**	**Peak position**	**FWHM**	**Area**	
LCO	796.69	3.16	6777	794.86	2.06	6724	781.22	3.06	13532	779.62	1.75	13428	1.01
LCRO82	796.07	3.08	6489	794.68	2.10	4318	780.68	3.01	12957	779.31	1.76	8621	1.50

Note: A line shape with 30% Lorentzian ratio was used for peak fitting. FWHM = full width at half maximum.

Table S5. The relative amount of the four different surface oxygen species of LCO and LCRO82. (Obtained from area under fitted XPS peaks).

	O^{2-}			O_2^{2-}/O^-			OH^-/O_2			H_2O		
Sample	**Peak position**	**FWHM**	**(At.)%**	**Peak position**	**FWHM**	**(At.)%**	**Peak position**	**FWHM**	**(At.)%**	**Peak position**	**FWHM**	**(At.)%**
LCO	528.74	1.18	43.53	530.22	1.69	16.16	531.28	1.35	30.27	532.25	1.59	10.04
LCRO82	528.78	1.20	43.95	530.16	1.82	23.57	531.31	1.42	24.08	532.42	1.65	8.41

Note: A line shape with 30% Lorentzian ratio was used for peak fitting. FWHM = full width at half maximum.

iv) Impedance data collection and analysis

The electrochemical impedance data has been collected at OCV voltage with Pt,Ru/C, LCO and LCRO82 as cathodes in Zinc-air batteries. The impedance data have been analyzed using ZSimpWin version 3.10 software and R(QR)(QR)W equivalent circuit is used for the fitting. **Figure S3,** shows the fitting of impedance data of Pt,Ru/C, LCO and LCRO82 catalysts and the values of fitted parameters are given in **table S6.**

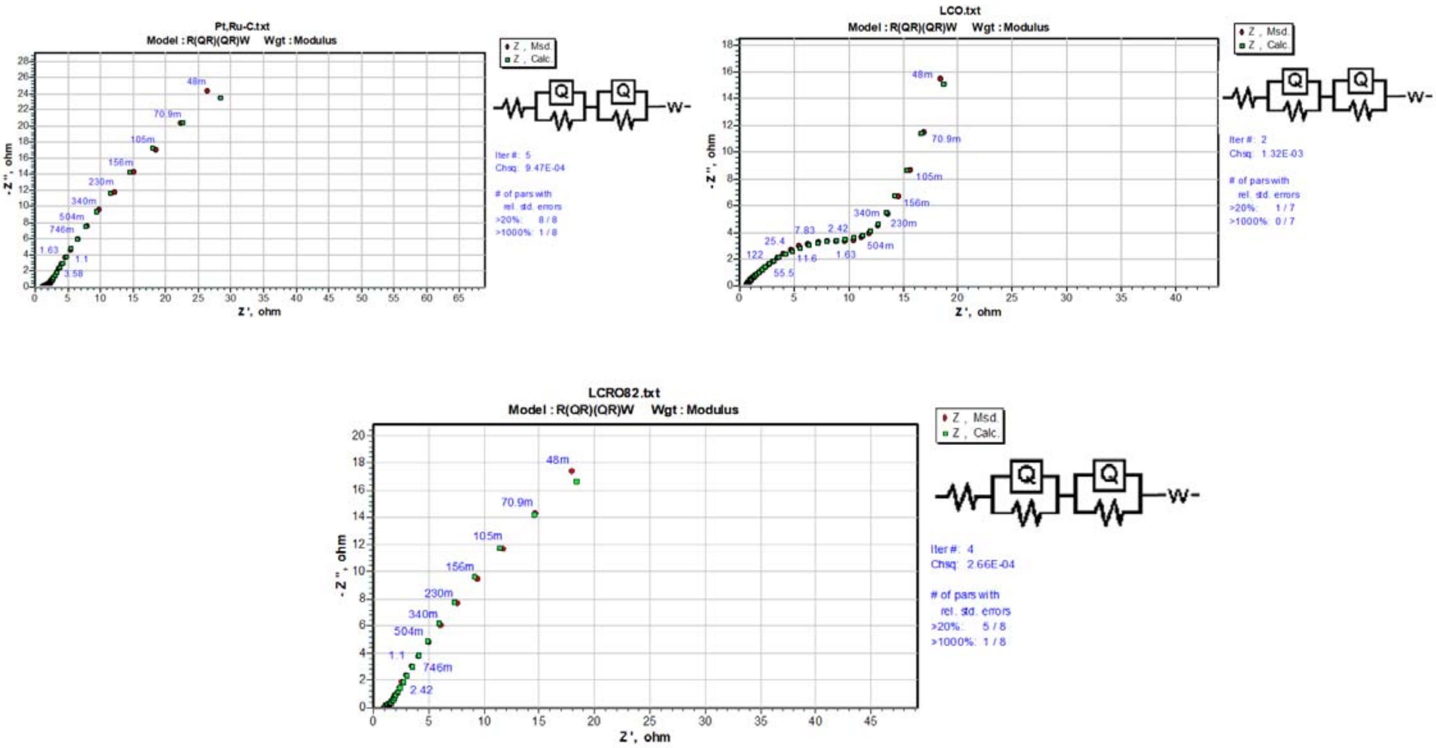

Fig. S3 Fitted Impedance spectra of Zn-air cell using Pt,Ru/C, LCO and LCRO82 catalysts at OCV voltage.

Table S6. Values of the R_s, R_{int} and R_{ct} obtained by simulated data of an impedance spectrum.

Sample	**R_s/ ohm**	**R_1/ ohm**	**R_2/ ohm**
LCO	0.53	0.88	10.4
LCRO82	1.03	0.40	0.54
Pt, Ru/C	0.95	0.44	1.51

Table S7. Comparison of bi-functional electrocatalytic activity of reported various perovskite electrocatalysts.

Catalyst	ORR Performance	OER performance	ΔE (V)	OER Tafel slope (mV dec^{-1})	Reference
LCRO82	$E_{j=3}$ - 0.63 V vs RHE	$E_{j=10}$ - 1.69 V vs RHE	1.06 V vs RHE	43	Our work
$La_{0.9}FeO_3$	$E_{j=3}$ - 0.38 V vs RHE	$E_{j=10}$ - 1.64 V vs RHE	1.26 V vs RHE	54	***Chem. Mater.*** *2016, 28, 1691–1697.*[2]
$LaNi_{0.8}Fe_{0.2}O_3$/VC	$E_{j=3}$ ≈ −0.64 vs RHE	$E_{j=10}$ ≈0.74 vs RHE	1.10 vs RHE	-	***J. Mater. Chem. A***, 2015,**3**, 9421-9426.[3]
$Ba_{0.5}Sr_{0.5}Co_{0.8}Fe_{0.2}O_{3-\delta}$	$E_{j=3}$ - 0.61 V vs RHE	$E_{j=10}$ - 1.73 V vs RHE	1.12 V vs RHE	129	***Adv. Mater.*** *2015, 27, 266–271.*[4]
$La_{0.5}Sr_{0.5}Co_{0.8}Fe_{0.2}O_3$	$E_{j=3}$ - 0.63 V vs RHE	$E_{j=10}$ - 1.82 V vs RHE	1.19 V vs RHE	-	***ChemSusChem*** *2015, 8, 1058–1065.*[5]
$La_{0.8}Sr_{0.2}Co_{1-x}Mn_xO_3$	$E_{j=3}$ - 0.70 V vs RHE	$E_{j=10}$ -1.73 V vs RHE	1.03 V vs RHE	113	***Electrochimica Acta,*** *254, (2017), 14-24.*[6]
$LaNi_{1-x}Mg_xO_3$	$E_{j=3}$ - 0.71 V vs RHE	$E_{j=10}$ -1.864 V vs RHE	1.15 vs RHE	-	***Journal of Power Sources,*** *265, (2014) 91-96.*[7]
$La_{0.8}Sr_{0.2}Mn_{1-x}Ni_xO_3$	$E_{j=3}$ - 0.71 V vs RHE	$E_{j=10}$ -1.87 V vs RHE	1.16 vs RHE	-	***ACS Appl. Mater. Interfaces*** *2016, 8, 10, 6520–6528.*[8]
Co-doped $LaMnO_3$/N-doped CNT	$E_{j=3}$ - -0.25 V vs SCE	$E_{j=11.7}$ - 0.76 V vs SCE	-	-	***Electrochemistry Comm.,*** *60, 2015, 38-41.*[9]
$La_{1-x}Y_xMnO_3$	E_{onset} -0.96 V vs. RHE	E_{onset} -1.65 V vs. RHE	-	-	***Energy,****154,2018, 561-570.*[10]
$La_{1.7}Sr_{0.3}Co_{0.5}Ni_{0.5}O4_{4+\delta}$	E_{onset} -0.696 V vs. RHE	$E_{j=11.7}$ - 1.85 V vs RHE	-	-	***Applied Surface Science,*** *2019, 464, 494-501.*[11]
$Pr_{0.5}Ba_{0.5}MnCo_{0.2}O_3$ nanofiber/VC	$E_{j=3}$ ≈0.70 vs. RHE	$E_{j=10}$ ≈1.83 vs. RHE	1.13	-	***ECS Transactions,*** *2016, 75, 955-964.*[12]

Table S8. The performance of rechargeable liquid Zn–air batteries with various perovskite electrocatalysts.

Catalyst	Current density (mA cm^{-2})	Overpotential (V)	Cyclic stability	Power Density (mW cm^{-2})	Reference
LCRO82	5	0.783	240 h, 1400 cycles	139	**Our work**
Pt/$Sr(Co_{0.8}Fe_{0.2})_{0.95}P_{0.05}O_{3-\delta}$	5	0.77	80 h, 240 cycles	*122*	***Advance Energy Materials,****2019,10,5,19 03271.*[13]
$Ba_{0.6}Sr_{0.4}Co_{0.79}Fe_{0.21}O_{2.67}$/$Ni_{0.6}Fe_{0.4}(OH)_x$ [NiFe]	5	0.89	100 cycles	52.8	***ACS Appl. Mater. Interfaces,*** *2019, 11, 39, 35853–35862.*[14]
$LaNiO_3$@FeOOH 1:1	5	0.86	16 h, 90 cycles	-	***Applied Catalysis B: Environmental,*** *262, (2020), 118291.*[15]
S-doped-LaCoO3	2	0.95	100 h, 300 cycle	92	***Chem. Mater.*** *2020, 32, 8, 3439–3446.*[16]
$Ce_{0.9}Gd_{0.1}O_{2-\delta}$ /$Pr_{0.5}Ba_{0.5}CoO_{3-\delta}$	10	0.98	200 h	207	***Applied Catalysis B: Environmental,*** *266 (2020) 118656.*[17]
$La_{0.9}MnO_{3-\delta}$	5	0.80	100 cycle	170	***Electrochimica Acta,*** *333 (2020) 135566.*[18]
Mg-doped-$LaNiO_3$	10	1.3	110 h	45	***ACS Appl. Energy Mater.*** *2019, 2, 1, 923–931.*[19]
$Ba_{0.5}Sr_{0.5}Co_{0.8}Fe_{0.2}O_{3-\delta}$	10	-	150 cycles	127	***ACS Nano*** *2017, 11, 11, 11594–11601.*[20]
Ag-doped-$Sm_{0.5}Sr_{0.5}CoO_{3-\delta}$	10	1.17	110 cycles	104	***Front. Chem.*** *2019, 7, 524.*[21]
MnO_2/$La_{0.7}Sr_{0.3}MnO_3$	10	0.949	100 cycles	181.4	***ACS Appl. Mater. Interfaces.*** *2019, 11, 25870.*[22]
$(La_{0.8}Sr_{0.2})_{0.95}Mn_{0.5}Fe_{0.5}O_3$	10	1.0	100 cycles	105	***Electrochimica Acta,*** *251 (2019) 113406.*[23]

Reference

1 Q. Shen, S. Li, G. Yang, B. Sunden and J. Yuan, *Energies*, 2019, **12**, 410.

2 Enhancing Electrocatalytic Activity of Perovskite Oxides by Tuning Cation Deficiency for Oxygen Reduction and Evolution Reactions | Chemistry of Materials, https://pubs.acs.org/doi/abs/10.1021/acs.chemmater.5b04457, (accessed June 23, 2020).

3 D. Zhang, Y. Song, Z. Du, L. Wang, Y. Li and J. B. Goodenough, *Journal of Materials Chemistry A*, 2015, **3**, 9421–9426.

4 Fabrication of Ba0.5Sr0.5Co0.8Fe0.2O3–δ Catalysts with Enhanced Electrochemical Performance by Removing an Inherent Heterogeneous Surface Film Layer - Jung - 2015 - Advanced Materials - Wiley Online Library, https://onlinelibrary.wiley.com/doi/full/10.1002/adma.201403897, (accessed June 23, 2020).

5 H. W. Park, D. U. Lee, M. G. Park, R. Ahmed, M. H. Seo, L. F. Nazar and Z. Chen, *ChemSusChem*, 2015, **8**, 1058–1065.

6 Q. Wang, Y. Xue, S. Sun, S. Li, H. Miao and Z. Liu, *Electrochimica Acta*, 2017, **254**, 14–24.

7 Z. Du, P. Yang, L. Wang, Y. Lu, J. B. Goodenough, J. Zhang and D. Zhang, *Journal of Power Sources*, 2014, **265**, 91–96.

8 Nickel-Doped La0.8Sr0.2Mn1–xNixO3 Nanoparticles Containing Abundant Oxygen Vacancies as an Optimized Bifunctional Catalyst for Oxygen Cathode in Rechargeable Lithium–Air Batteries | ACS Applied Materials & Interfaces, https://pubs.acs.org/doi/abs/10.1021/acsami.6b00296, (accessed June 23, 2020).

9 D. U. Lee, M. G. Park, H. W. Park, M. H. Seo, V. Ismayilov, R. Ahmed and Z. Chen, *Electrochemistry Communications*, 2015, **60**, 38–41.

10 H. Miao, Z. Wang, Q. Wang, S. Sun, Y. Xue, F. Wang, J. Zhao, Z. Liu and J. Yuan, *Energy*, 2018, **154**, 561–570.

11 P. Li, B. Wei, Z. Lü, Y. Wu, Y. Zhang and X. Huang, *Applied Surface Science*, 2019, **464**, 494–501.

12 Y. Zhang, Y.-F. Sun and J.-L. Luo, *ECS Trans.*, 2016, **75**, 955.

13 X. Wang, J. Sunarso, Q. Lu, Z. Zhou, J. Dai, D. Guan, W. Zhou and Z. Shao, *Advanced Energy Materials*, 2020, **10**, 1903271.

14 R. Majee, Q. A. Islam and S. Bhattacharyya, *ACS Appl. Mater. Interfaces*, 2019, **11**, 35853–35862.

15 Z. Li, L. Lv, X. Ao, J.-G. Li, H. Sun, P. An, X. Xue, Y. Li, M. Liu, C. Wang and M. Liu, *Applied Catalysis B: Environmental*, 2020, **262**, 118291.

16 Modulation of Electronics of Oxide Perovskites by Sulfur Doping for Electrocatalysis in Rechargeable Zn–Air Batteries | Chemistry of Materials, https://pubs.acs.org/doi/abs/10.1021/acs.chemmater.9b05148, (accessed June 23, 2020).

17 L. Gui, Z. Wang, K. Zhang, B. He, Y. Liu, W. Zhou, J. Xu, Q. Wang and L. Zhao, *Applied Catalysis B: Environmental*, 2020, **266**, 118656.

18 H. Miao, X. Wu, B. Chen, Q. Wang, F. Wang, J. Wang, C. Zhang, H. Zhang, J. Yuan and Q. Zhang, *Electrochimica Acta*, 2020, **333**, 135566.

19 J. Bian, R. Su, Y. Yao, J. Wang, J. Zhou, F. Li, Z. L. Wang and C. Sun, *ACS Appl. Energy Mater.*, 2019, **2**, 923–931.

20 Y. Bu, O. Gwon, G. Nam, H. Jang, S. Kim, Q. Zhong, J. Cho and G. Kim, *ACS Nano*, 2017, **11**, 11594–11601.

21 Y. Zhang, Y. Guo, T. Liu, F. Feng, C. Wang, H. Hu, M. Wu, M. Ni and Z. Shao, *Front. Chem.*, , DOI:10.3389/fchem.2019.00524.

22 S. Yan, Y. Xue, S. Li, G. Shao and Z. Liu, *ACS Appl. Mater. Interfaces*, 2019, **11**, 25870–25881.

23 R. Yuan, Y. He, W. He, M. Ni and M. K. H. Leung, *Applied Energy*, 2019, **251**, 113406.